https://doi.org/10.3311/PPee.39922

Periodica Polytechnica Electrical Engineering and Computer Science, 69(3), pp. 305–317, 2025

Diverse Emperor Penguin Algorithm for Partially Shaded PV Array Reconfiguration

Anil Marneni[1], Pravin Murugesan[1], Sowthily Chandrasekharan[2], Muhilan Paramasivam[3], Senthil Kumar Subramaniam[1*]

[1] Department of Electrical and Electronics Engineering, National Institute of Technology, 620015 Tiruchirappalli, India
[2] Department of Electrical and Electronics Engineering, Rohini College of Engineering and Technology, Kanyakumari, 629401 Tamil Nadu, India
[3] Department of Electrical and Electronics Engineering, Mount Zion College of Engineering and Technology, Pudukkottai, 622507 Tamil Nadu, India
* Corresponding author, e-mail: skumar@nitt.edu

Received: 20 January 2025, Accepted: 26 May 2025, Published online: 14 July 2025

Abstract

A significant challenge in the operation of Photo-Voltaic (PV) array is partial shading, which drastically reduces the power output. Shaded arrays exhibit numerous local Maximum Power Point (LMPP) alongside a single Global Maximum Power (GMP). Reconfiguring shaded modules to extract the GMP is crucial, and achieving this relies heavily on a uniform shadow distribution across the PV surface. This paper proposes a novel strategy, Diverse Emperor Penguin (DEP) algorithm, for uniform shadow distribution across shaded PV arrays. It is a onetime static reconfiguration technique based on the commonly occurring shading patterns in a given location. The proposed strategy was tested on 9 × 9 PV array at ten distinct shading patterns in MATLAB/Simulink platform. The analytical results observe the power enhancement at all the shading patterns and highest power improvement is 23.01%, 10.20% when compared with standard TCT and SuDoKu configurations respectively. The same were tested experimentally on 3 × 3 PV array and compared with standard TCT and SuDoKu configurations and the results obtaind confirm that the proposed technique has superior performance compared with stated techniques.

Keywords

solar PV systems, diverse penguin algorithm, static reconfiguration, power enhancement, mismatch losses

1 Introduction

The significant enhancement in global energy demands and greenhouse gas emissions contributing to global warming, adoption of renewable energy sources (RES) across various engineering fields have substantially increased [1, 2]. Among, solar photovoltaic (PV) power generation has gained prominence across the world, since it is very sustainable and cost effective [3–5]. PV generation is used in many applications of CO_2 capture cycle [6], an integrated structure for liquid hydrogen production [7] and liquefied natural gas production etc. [8] and it offers several advantages, including minimal maintenance requirements, reduced carbon emissions, and quiet operation. However, despite its advantages, solar energy faces significant challenges, such as its intermittent availability and non-linear, environmentally dependent power output [9].

Further, photovoltaic modules can suffer from partial shading (PS) due to factors like clouds, nearby structures, dust, and dirt etc. [10]. The shading effect will increase mismatch losses and reduce the power output of the solar PV array. In a quest to get the maximum PV power output under partial shading conditions, the authors of [11, 12] undertook a comprehensive evaluation of various topologies, including series, parallel, series-parallel, Total-Cross-Tied (TCT), bridge link (BL), and honeycomb (HC). This analysis revealed that the TCT configuration demonstrably outperformed the others for most of the PS conditions.

To prevent the PS effect, at preliminary stages bypass diodes are used across the modules and it has limited advantages, overheating, power losses and multiple peaks occur in the Power Voltage (P-V) characteristics of the array. Later, various metaheuristic optimization

Cite this article as: Marneni, A., Murugesan, P., Chandrasekharan, S., Paramasivam, M., Subramaniam, S. K. "Diverse Emperor Penguin Algorithm for Partially Shaded PV Array Reconfiguration", Periodica Polytechnica Electrical Engineering and Computer Science, 69(3), pp. 305–317, 2025.
https://doi.org/10.3311/PPee.39922

algorithms, dynamic and static reconfiguration techniques are employed. Metaheuristic optimization is popular since it is easy to implement and by pass the local optima problem [13]. Deshkar et al. implemented genetic algorithm (GA) on solar PV array to extract maximum power [14]. In this, uniform shadow distribution of array achieved by changing the electrical connections of modules keeping physical location of modules unchanged. Later, sudhakar Babu et al. introduced particle swarm optimization (PSO) to relocate the PV modules subjected to shadow with improving the output power [15]. Fathy Ahmed proposed a method utilizing the Grasshopper Optimization Algorithm (GOA) for reconfiguring shaded PV arrays to maximize power generation [16]. In response to the challenge posed by partial shade on large-scale photovoltaic arrays, Yousri et al. [17] proposed a modified Harris Hawk Optimization (HHO) algorithm for reconfiguring shaded panels to maximize power output. In terms of optimizing the switching matrix design, explores three distinct algorithms: The Flow Regime Algorithm (FRA), the Social Mimic Optimization algorithm (SMO), and the Rao optimization algorithm [18]. These methods have been tested and compared on 9 × 9 array, at different traditional shading patterns of short and wide shadow, long and narrow shadow etc. and FRA technique achieved highest power enhancement and lowest mismatch losses. However, metaheuristic optimization algorithms require higher computational time and space, when the size of the solar PV array increases.

To reduce the heat losses and increase the power output of solar PV array, various dynamic reconfiguration techniques are familiar since it need not change its physical location and reduce the shading effect based on electrical connections of the PV array. Tabanjat et al. have recommended the reconfiguration for shaded PV panels, using switching control of solar PV array [19]. In this, fuzzy logic (FL) estimator identifies percentage of shading, faulty panel and then switching controller compares PV panel's output and decides the changing of the panels through switches. Further, Sanseverino et al. implement dynamic programming algorithm for changing the switches layout of PV array, under shading conditions [20]. This dynamic reconfiguration mitigates the mismatch losses and increases the power output of solar PV array under non-homogeneous conditions. Yousri et al. introduced marine predators' algorithm (MPA) to restructure the PV array dynamically under partial shading conditions [21]. It introduces a novel objective function to improve the power output of the solar PV array. It is tested on large scale solar PV array of 16 × 16 and 25 × 25, compared with a regular TCT connection and several optimization techniques. However, dynamic reconfiguration requires extra controlled switches, sensors and the cost of the system will be increased.

To reduce the computational burden and cost of the system, static reconfiguration techniques are proposed, and it will improve the performance of the solar PV array [22–29]. In this static reconfiguration, the shading effect will be reduced by shifting the PV panels without changing their electrical connections. Mishra et al. [22] proposed a novel structure (NS) of the PV array for reducing the mismatch losses and improve the power output of solar PV array. It is tested and compared on 6 × 4 sizes of TCT, series-parallel TCT (SP-TCT), bridge link-TCT (BL-TCT) etc. at diagonally shading and other shading patterns also. Further, Horoufiany and Ghandehari [23] proposed Sudoku puzzle pattern with adding dispersion rules for mutual shading effect (MSE) on solar PV array. It will reduce the MSE of the PV plant collector of same tilt and direction. It is tested and compared on 9 × 9 PV array with non-optimized Sudoku puzzle. Later, Akrami and Pourhossein [24] proposed a novel power comparison technique (PCT) to optimize power output from PV arrays. In this, PCT finds absolute peak, by comparing the peaks of the power voltage (P-V) characteristics of the solar PV array, tested on SP and TCT configurations and observed power enhancement compared with state of art works. Belhaouas et al. [25] address shading by proposing three physical configurations that maximize the distance between neighboring panels within a PV array. In this, modules in different rows and columns are arranged such that, the shading pattern distributed resulting in an increase in each row current. It is tested on traditional shading patterns of Short and Narrow, Short and Wide, Wide and Long etc. There is an interconnection of modules in a TCT configuration, to distribute the shading effect evenly in each row such that the power output of solar PV array is improved [26, 27]. Further, Sai Krishna and Tukaram proposed two puzzle patterns namely, Ken-Ken and Skyscraper [28] for TCT connected shaded PV arrays and odd-even structure of TCT configuration proposed by Nasiruddin et al. [29] to redistribute the shading effect such that it improves the solar PV array performance.

In the quest for simpler and faster algorithms to overcome limitations in existing reconfiguration methods, research is underway to develop more efficient algorithms. This paper proposes a novel strategy, Diverse Emperor Penguin (DEP) algorithm, for uniform shadow

distribution across shaded PV arrays. It is a one-time static reconfiguration technique based on the commonly occurring shading patterns in a location. The proposed strategy aims to maximize the generated power of the target array, while minimizing the disparity between the highest and lowest row current levels. This DEP algorithm is employed to analyze a 9 × 9 PV array under various shading scenarios. To assess the effectiveness of the proposed approach, DEP's results are compared with existing SuDoKu and TCT algorithms, using a range of statistical metrics. The findings demonstrate that DEP algorithm is superior in achieving the highest power outputs and favorable PV characteristics.

2 System description

There are various solar PV array configurations available: Series (S), Parallel (P), Series-Parallel (SP), Total cross Tied (TCT), Bridge Link (BL) and Honey-Comb (HC). The Total Cross-Tied (TCT) configuration reigns supreme in achieving rated power output compared with remaining configurations [11]. The 9 × 9 TCT PV array connection is shown in Fig. 1

In TCT configuration, the row current can be evaluated by:

$$I_{Ri} = \left(\frac{G_{in1}}{G_0}\right) I_m + \ldots\ldots\ldots\ldots + \left(\frac{G_{inj}}{G_0}\right) I_m, \tag{1}$$

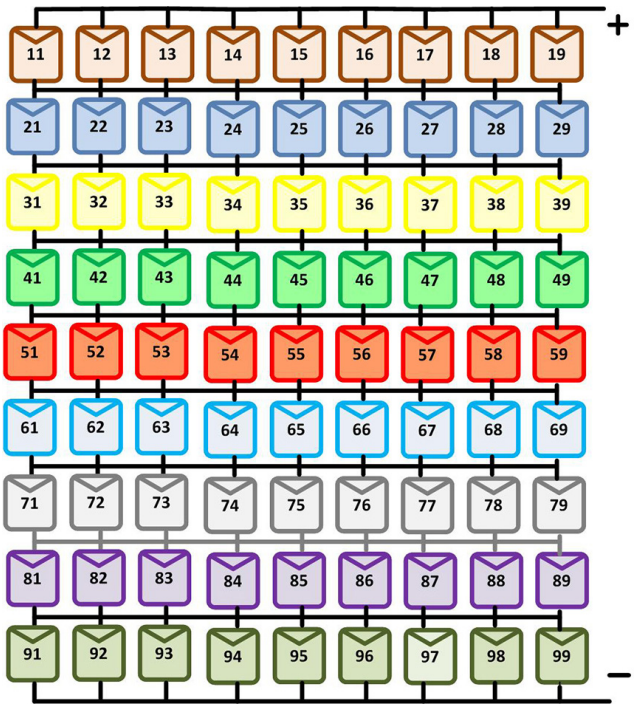

Fig. 1 TCT 9 × 9 PV array configuration

where:

- i, j are row and column respectively,
- I_m = Maximum row current at standared irradiance (1000 W/m^2) and 25 °C,
- G_{in} = insolation level of the panel,
- G_0 = standared irradiance or insolation level of the panel.

The total solar PV array current is represented in Eq. (2) and where p is the total number of rows.

$$I_{\text{PV}} = \sum_{i=1}^{p} I_{Ri}, \tag{2}$$

3 Proposed Diverse Emperor Penguin algorithm

Inspiration from Emperor Penguin (EP) optimization, we are proposing diverse emperor penguin (DEP) algorithm to reduce the mismatch losses and output power enhancement at frequently occurring shading patterns in a location. In DEP, the penguin movement is dependent on atmospheric changes in any location and can be updated by using:

$$P_{\text{mov+1}} = P_{\text{mov}} + \vec{A}D, \tag{3}$$

where:

- $P_{\text{mov+1}}$ is the next position of penguin,
- P_{mov} is the present position of penguin,
- D is the distance between the penguins,
- $\vec{A}$ is the vector to decide the penguin's movement.

DEP Algorithm involves utilizing information gained from the current position of each penguin before relocating it. This modification constructs an information using a threshold selected from the interval [0,1]. Its movement decided by the vector such that the distance between the penguins should be reduced.

3.1 DEP for partial shading

The DEP strategy is applied for partial shading problem in the solar PV array and the flowchart for the proposed DEP algorithm is shown in Fig. 2.

In this for one particular shading, firstly the column shift to their 'number' of times. For example, the n^{th} column shifted 'n' number of times and form the shading matrix. At this check the shading matrix achieving higher power improvement and less mismatch losses. It is a one time reconfiguration technique for the predefined shading patterns. The DEP algorithm for the TCT configuration is shown in Fig. 3

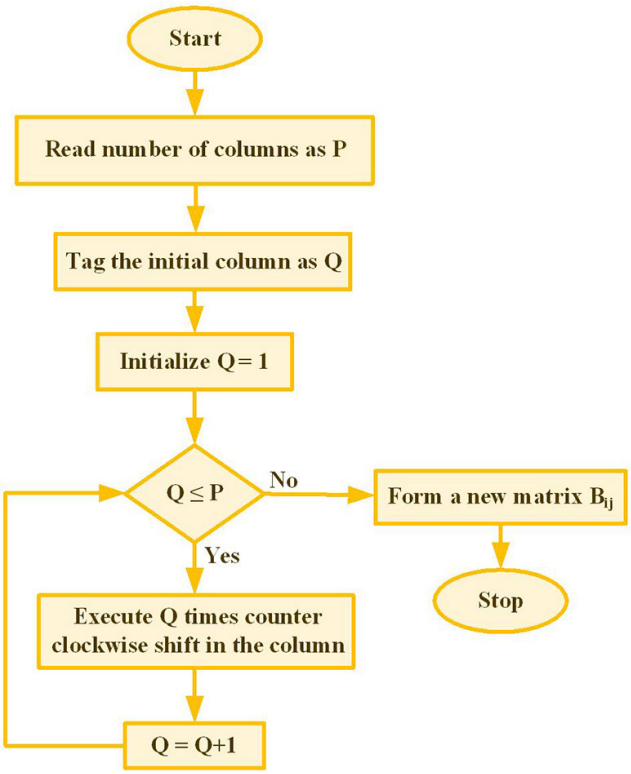

Fig. 2 Flow chart of DEP

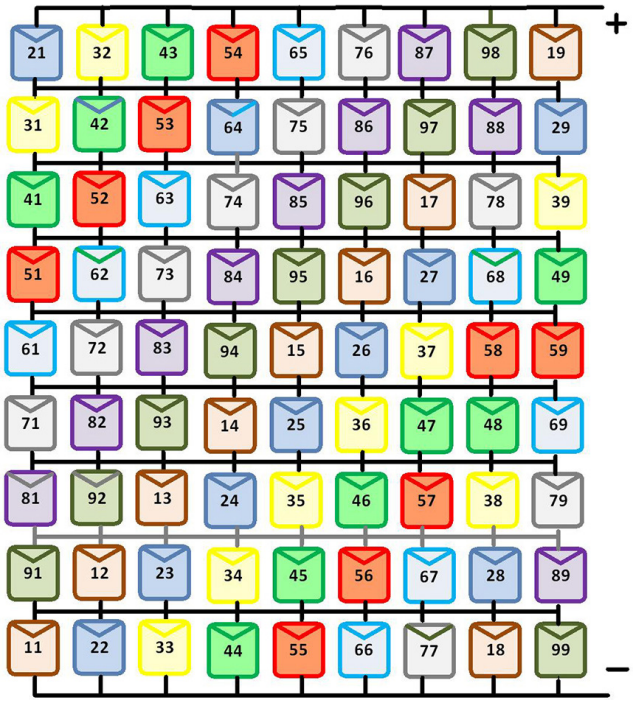

Fig. 3 Proposed DEP algorithm on TCT configuration

4 Simulation results and discussions

To validate the performance of the proposed strategy a 9 × 9 TCT PV array is employed as shown in Fig. 1 and the specifications of PV panel are shown in Table 1.

Table 1 Solar PV panel specifications at standard test conditions

Parameter	Value (Single Panel)
Rated peak power	79.2 W
Voltage at Maximum Power (V_{mp})	18 V
Current at Maximum Power (I_{mp})	4.4 A
Open-circuit voltage (V_{oc})	22.1 V
Short circuit current (I_{sc})	4.8 A

The proposed strategy evaluates the performance under various shading scenarios on a 9 × 9 PV array using MATLAB/Simulink software [30]. The shading scenarios ranging from 1000 W/m² to 100 W/m², with a 4 × 4, 4 × 3, and 3 × 5 shadow cast upon the array surface is demonstrated. All testing shadows are like traditional short and wide type shading. To quantify the effectiveness of each approach, this paper employs several statistical metrics:

1. percentage power enhancement,
2. mismatch power loss,
3. percentage power loss, and,
4. fill factor.

4.1 Shading Pattern I

In this instance, a 300 W/m², 400 W/m² and 700 W/m², shade covers the lower left corner of 4 × 4 array. The remaining PV modules in the 9 × 9 array got full irradiation, 1000 W/m², as shown in Fig. 4 (a). The generated scattered shade patterns examined for the TCT scheme, employing for SuDoKu and proposed DEP, are illustrated in Figs. 4 (b) and (c), respectively. Fig. 5 shows the P-V (Power-Voltage) characteristics of shading Pattern I.

4.2 Shading Pattern II

In this shading pattern, the irradiance levels 300 W/m², 600 W/m² are applied to specific regions of a 4 × 3 array in the lower right corner of 9 × 9 PV array as shown in Fig. 6 (a). The reconfigured shade patterns generated by the SuDoKu and DEP are illustrated in Fig. 6 (b) and (c).

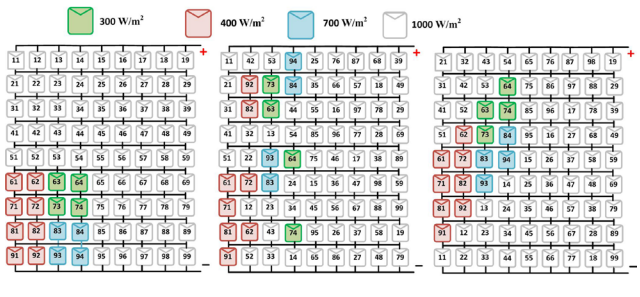

Fig. 4 Pattern I reconfiguration for (a) TCT, (b) SuDoKu, (c) and DEP

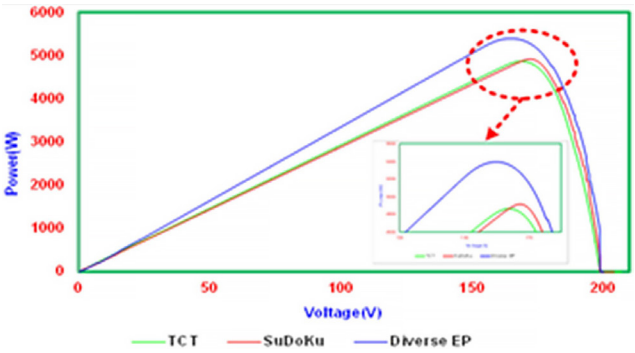

Fig. 5 P-V characteristics for Pattern I

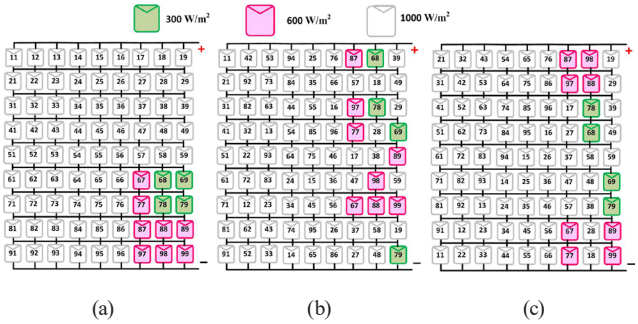

(a) (b) (c)

Fig. 6 Pattern II reconfiguration for (a) TCT, (b) SuDoKu, (c) and DEP

The DEP demonstrates reduced power variations, leading to improved overall power output stability.

Fig. 7 presents the P-V curves for the TCT and dispersed shading patterns of SuDoKu and DEP. Based on these characteristics, the GMPP (Global Maximum Power Point) achieved using DEP, SuDoKu, and TCT are 5711 W, 5577 W, and 5225 W, respectively. The simulated GMPP values within the MATLAB environment suggest a substantial power gain with the proposed DEP. The SuDoKu approach follows closely with a power generation of 5577 W.

4.3 Shading Pattern III

In this shading pattern, the PV array's top left corner of 4 × 4 is shaded, and the irradiation profiles taken into account are 100 W/m², 200 W/m², 300 W/m² and 500 W/m², as shown in Fig. 8 (a). Its SuDoKu and DEP shade patterns are shown in Figs. 8 (b) and (c), respectively.

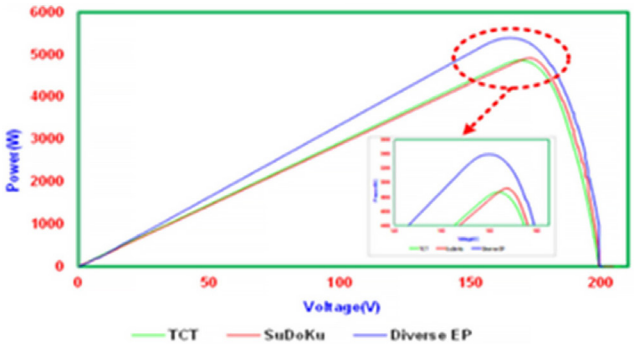

Fig. 7 P-V characteristics for Pattern II

The extracted power from the proposed DEP is 4860 W, which is significantly more than the other two layouts. Fig. 9 displays the P-V curves that resemble the Pattern III. After a successful reconfiguration, the power output of TCT, SuDoKu, and DEP is 4365 W, 4573 W and 4860 W respectively.

4.4 Shading Pattern IV

In this instance, four different irradiations were considered to demonstrate the usefulness of the proposed strategy. As seen in Fig. 10 (a), the 4 × 4 PV array is shaded with irradiation levels of 200 W/m², 300 W/m², 400 W/m², and 600 W/m², while other modules receive

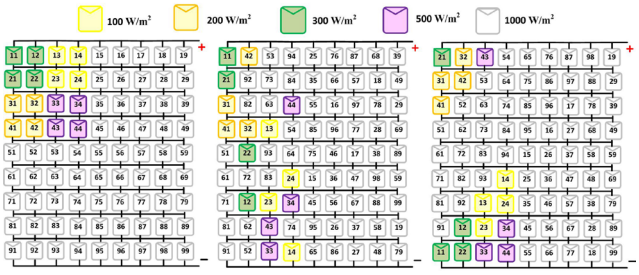

(a) (b) (c)

Fig. 8 Pattern III reconfiguration for (a) TCT, (b) SuDoKu, (c) and DEP

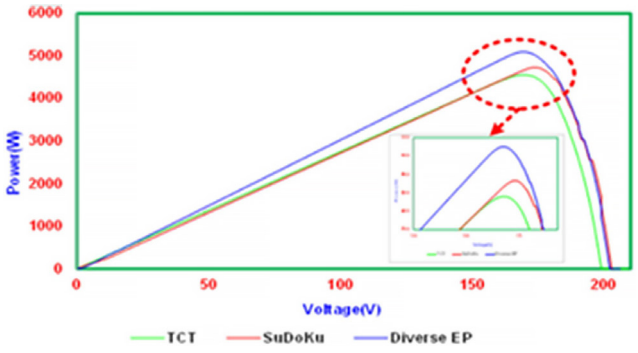

Fig. 9 P-V characteristics for Pattern III

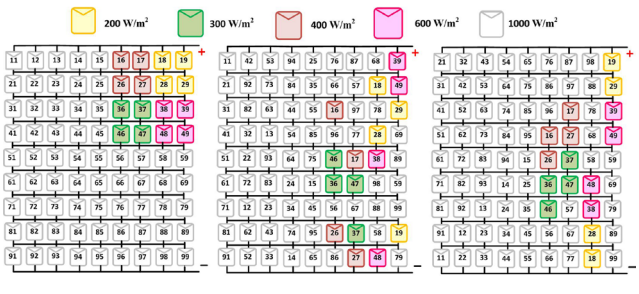

(a) (b) (c)

Fig. 10 Pattern IV reconfiguration for (a) TCT, (b) SuDoKu, (c) and DEP

full irradiation of 1000 W/m^2. The suggested DEP and the SuDoKu dispersed shade patterns are shown in Figs. 10 (b) and (c), respectively.

Fig. 11 presents the simulated P-V curves for the shading Pattern IV. It is interesting to point out that the reconfigured DEP approach has demonstrated its maximal power even at a short wide shadow pattern from the plotted curves. The proposed DEP in this pattern generates 5284 W power, which is more than TCT and SuDoKu, respectively.

4.5 Shading Pattern V

In this shading pattern, the irradiation profiles of PV array are considered is 100 W/m^2, 200 W/m^2, 700 W/m^2 and 1000 W/m^2, as shown in Fig. 12 (a). Additionally, its SuDoKu and DEP shade patterns are shown in Figs. 12 (b) and (c), respectively.

Fig. 13 displays the P-V curves, that resemble the shading Pattern V. After a successful reconfiguration, the power output of TCT, SuDoKu, and DEP is 4161 W, 4656 W and 4828 W respectively.

4.6 Shading Pattern VI

In this instance, four different irradiations are considered to demonstrate the usefulness of the proposed strategy.

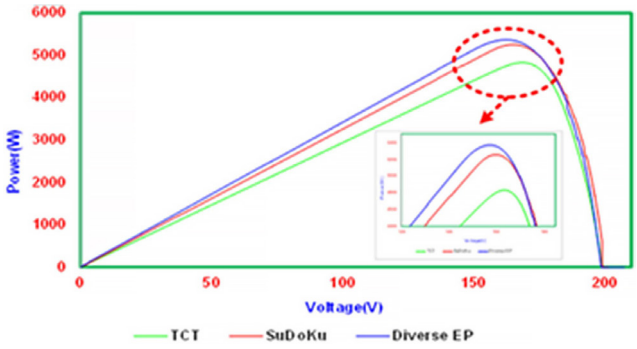

Fig. 11 P-V characteristics for Pattern IV

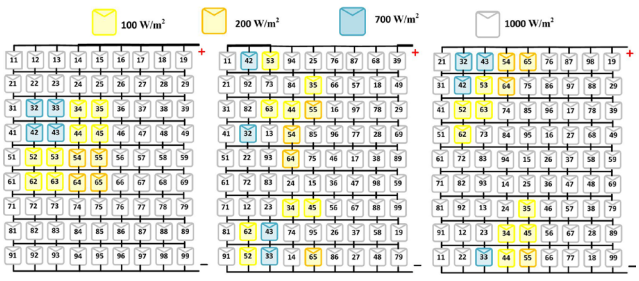

(a) (b) (c)

Fig. 12 Pattern V reconfiguration for (a) TCT, (b) SuDoKu, (c) and DEP

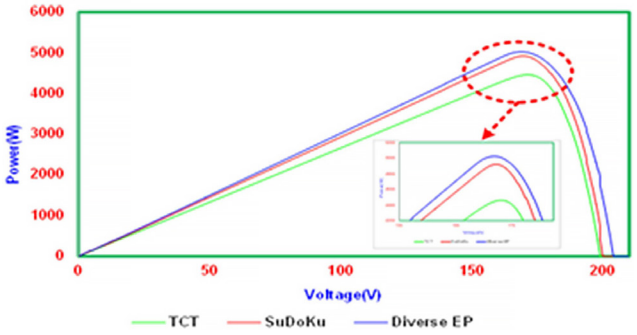

Fig. 13 P-V characteristics for Pattern V

As seen in Fig. 14 (a), the 4 × 4 PV array is shaded with irradiation levels of 100 W/m^2, 600 W/m^2, and 700 W/m^2, while other modules receive full irradiation of 1000 W/m^2. The suggested DEP and the SuDoKu dispersed shade patterns are shown in Figs. 14 (b) and (c), respectively. The proposed DEP generates 5194 W power, which is more than TCT and SuDoKu, respectively.

Fig. 15 Presents the simulated P-V curves for this shading pattern.

4.7 Shading Pattern VII

In this shading pattern, there are 200 W/m^2, 300 W/m^2, 500 W/m^2 and 700 W/m^2, while other modules receive irradiation of 1000 W/m^2 as shown in Fig. 16 (a). The generated scattered shade patterns for the examined TCT

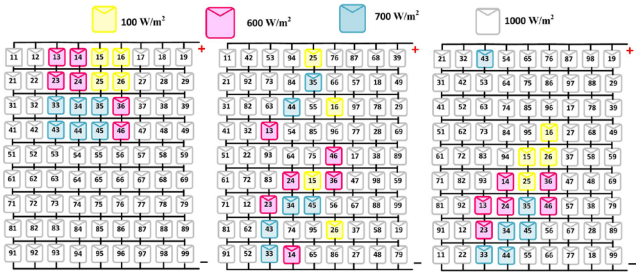

(a) (b) (c)

Fig. 14 Pattern VI reconfiguration for (a) TCT, (b) SuDoKu, (c) and DEP

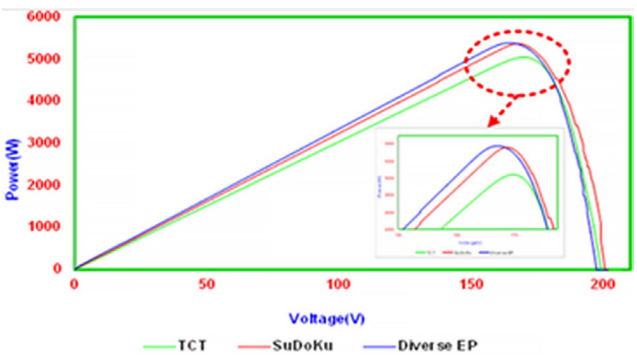

Fig. 15 P-V characteristics for Pattern VI

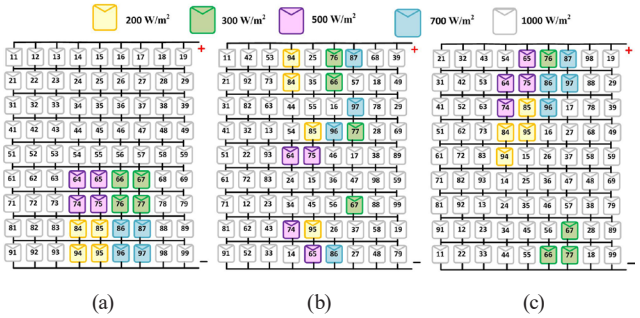

(a) (b) (c)

Fig. 16 Pattern VII reconfiguration for (a) TCT, (b) SuDoKu, (c) and DEP

scheme employing SuDoKu and the suggested DEP are illustrated in Figs. 16 (b) and (c), respectively.

Fig. 17 displays the P-V curves that resemble Pattern VII. After a successful reconfiguration, the power output of TCT, SuDoKu, and DEP are 4571 W, 5012 W and 5254 W respectively.

4.8 Shading Pattern VIII

As seen in Fig. 18 (a), the 4 × 4 PV array is shaded with irradiation levels of 100 W/m², 300 W/m², 400 W/m² and 600 W/m², while other modules receive full irradiation of 1000 W/m².

The suggested DEP and the SuDoKu dispersed shade patterns are shown in Figs. 18 (b) and (c), respectively.

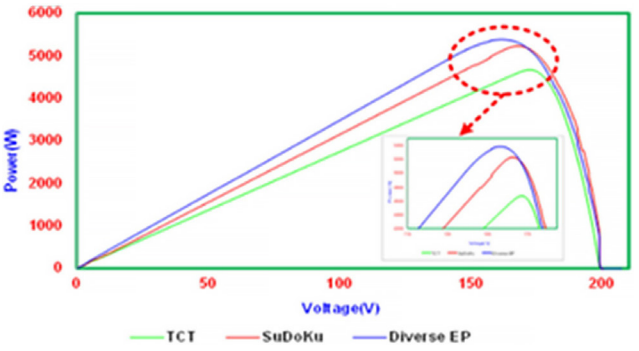

Fig. 17 P-V characteristics for Pattern VII

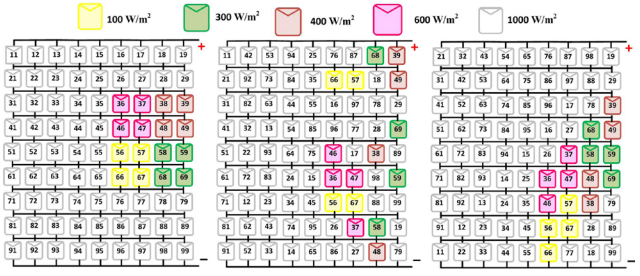

(a) (b) (c)

Fig. 18 Pattern VIII reconfiguration for (a) TCT, (b) SuDoKu, (c) and DEP

The proposed DEP generates 4941 W power, which is more than TCT and SuDoKu, respectively. Fig. 19 presents the simulated P-V curves for this shading pattern.

4.9 Shading Pattern IX

In this pattern, a 100 W/m², 200 W/m², 600 W/m² and 800 W/m², while other modules receive irradiation of 1000 W/m² as shown in Fig. 20 (a). The generated scattered shade patterns for the examined TCT scheme, SuDoKu and the suggested DEP are illustrated in Figs. 20 (b) and (c), respectively.

Fig. 21 displays the P-V curves that resemble Pattern XI. The power output of TCT, SuDoKu, and DEP is 4786 W, 4880 W and 5378 W respectively.

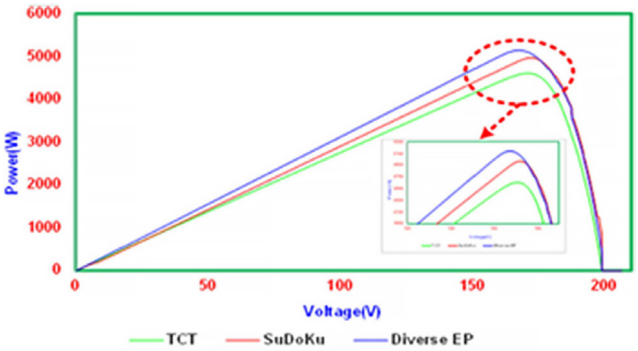

Fig. 19 P-V characteristics for Pattern VIII

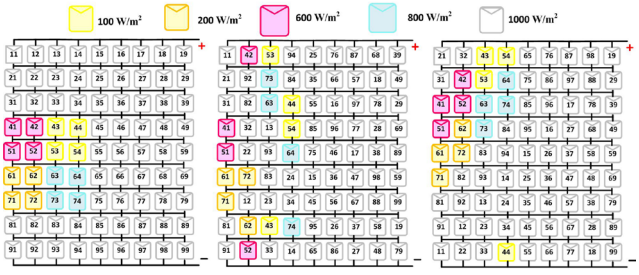

(a) (b) (c)

Fig. 20 Pattern IX reconfiguration for (a) TCT, (b) SuDoKu, (c) and DEP

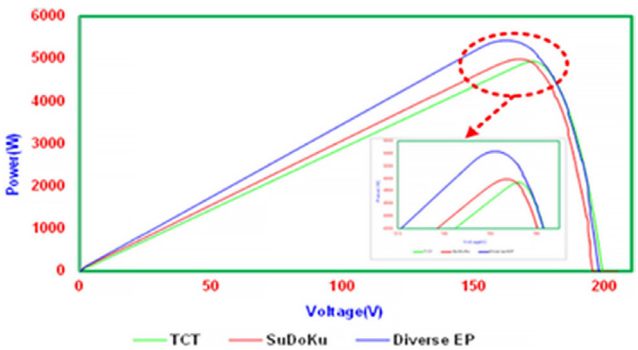

Fig. 21 P-V characteristics for Pattern IX

4.10 Shading Pattern X

The 9 × 9 PV array, considered irradiation profiles are 200 W/m^2, 400 W/m^2, 600 W/m^2 and 1000 W/m^2, as shown in Fig. 22 (a) Its SuDoKu and DEP shading patterns are shown in Figs. 22 (b) and (c), respectively. Fig. 23 displays the P-V curves that resemble this shading pattern.

After successful reconfiguration, the power output of TCT, SuDoKu, and DEP is 4140 W, 4808 W and 5093 W respectively.

5 Performance measures

A critical analysis is conducted to evaluate the effectiveness of the suggested technique by considering several performance parameters, including mismatch power loss, fill factor, percentage of power loss, and percentage of power augmentation between each technique. A synoptic perspective is provided to help comprehend the impact of reconfiguration under shadow conditions. The proposed DEP, TCT, and SuDoKu are computed and compared in Table 2 with the current, voltage, power, fill factor, power loss, mismatch loss and the performance ratio for the ten different shading patterns.

5.1 Power enhancement

The power generation in basic TCT, SuDoKu and proposed DEP at ten different shading patterns has been observed in Fig. 24. At all the shading patterns, power enhancement has been observed with the proposed method

and highest power enhancement in Pattern-X with 23.01%, 10.2% in Pattern-IX when compared with basic TCT and SuDoKu respectively.

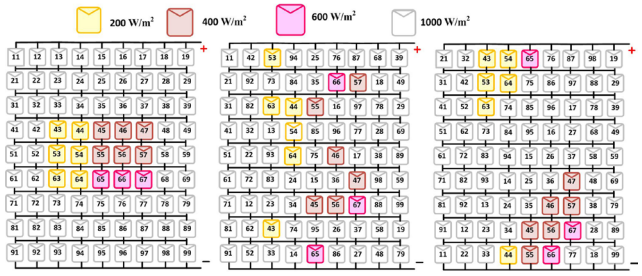

Fig. 22 Pattern X reconfiguration for (a) TCT, (b) SuDoKu, (c) and DEP

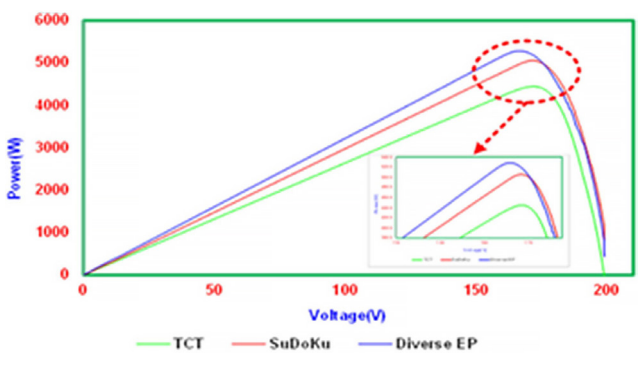

Fig. 23 P-V characteristics for Pattern X

5.2 Mismatch loss

These losses typically happen when PV modules fail to operate at their maximum power capacity. This demonstrates that losses in mismatch power indicate a significant decrease in output power. Fig. 25 shows the mismatch loss for different pattern configurations. With the proposed DEP, the highest mismatch loss reduction occurred in Pattern IV of 64.03%, lowest power reduction in Pattern III of 41.7% when compared with basic TCT configuration. This percentages would be 57.63%, 15.72% in Pattern IX and V respectively when compared with SuDoKu configuration.

5.3 Power loss

Estimating the percentage of power loss in each technique is essential to understanding the precise losses in the system. Fig. 26 shows the power losses in all ten different shading patterns with the proposed method along with basic TCT and SuDoKu configurations. The highest power loss reduction occurred in Pattern X of 40.72%, and lowest is 23.4% in Pattern III with the proposed method when compared with basic TCT configuration. The same is compared with SuDoKu and the values are 31.12%, 9.42% in Pattern IX, Pattern V respectively.

5.4 Fill factor

The crucial factor for assessing the performance of PV plants is the fill factor. Fig. 27 displays the calculated fill factors for the three configurations. With the proposed method, the highest performance improvement has been observed in Pattern X and IX when compared with basic TCT and SuDoKu configurations. In this the fill factors increase from 0.482 to 0.593, 0.568 to 0.626 respectively. After analyzing all performance parameters, the proposed DEP method gives better performance at Pattern X and IX when compared with basic TCT configuration and SuDoKu respectively. However, in the case of highly rated PV plants, the slight difference could result in a high level. The combination of the suggested DEP and SuDoKu (SDU) approach results in less power augmentation due to the SDU method's limitations. This demonstrates the capability of introducing the DEP-reconfiguration approach to provide the better reconfiguration topology.

Table 2 Comparative analysis of proposed DEP algorithm at ten different shading patterns

Shading Pattern	Configuration	Voltage (V)	Current (A)	Power (W)	Power Loss	Mismatch Loss	Fill Factor	Performance Ratio
	Proposed DEP	161.4	31.68	5113	1367	663	0.595	0.789
Pattern I	SuDoKu	161.1	29.48	4749	1731	1027	0.553	0.733
	TCT	160.8	28.16	4528	1952	1248	0.527	0.699
	Proposed DEP	158.3	36.08	5711	769	289	0.665	0.881
Pattern II	SuDoKu	158	35.3	5577	903	423	0.649	0.861
	TCT	158.2	33.03	5225	1255	775	0.608	0.806
	Proposed DEP	161.8	30.04	4860	1620	692	0.566	0.750
Pattern III	SuDoKu	159.9	28.6	4573	1907	979	0.532	0.706
	TCT	158.6	27.52	4365	2115	1187	0.508	0.674
	Proposed DEP	160.6	32.9	5284	1196	396	0.615	0.815
Pattern IV	SuDoKu	160.2	31.98	5123	1357	557	0.596	0.791
	TCT	160.1	28.6	4579	1901	1101	0.533	0.707
	Proposed DEP	161.2	29.95	4828	1652	922	0.562	0.745
Pattern V	SuDoKu	160	29.1	4656	1824	1094	0.542	0.719
	TCT	159.8	26.04	4161	2319	1589	0.484	0.642
	Proposed DEP	157.4	33	5194	1286	662	0.604	0.802
Pattern VI	SuDoKu	157.3	32.12	5052	1428	804	0.588	0.780
	TCT	157	29.7	4663	1817	1193	0.543	0.720
	Proposed DEP	158.6	33.13	5254	1226	490	0.611	0.811
Pattern VII	SuDoKu	158.2	31.68	5012	1468	732	0.583	0.773
	TCT	157.4	29.04	4571	1909	1173	0.532	0.705
	Proposed DEP	160.2	30.84	4941	1539	707	0.575	0.763
Pattern VIII	SuDoKu	159.7	29.17	4658	1822	990	0.542	0.719
	TCT	158.6	26.9	4266	2214	1382	0.496	0.658
	Proposed DEP	156.7	34.32	5378	1102	366	0.626	0.830
Pattern IX	SuDoKu	156.2	31.24	4880	1600	864	0.568	0.753
	TCT	155.4	30.8	4786	1694	958	0.557	0.739
	Proposed DEP	161.2	31.6	5093	1387	619	0.593	0.786
Pattern X	SuDoKu	160.7	29.92	4808	1672	904	0.560	0.742
	TCT	160.5	25.8	4140	2340	1572	0.482	0.639

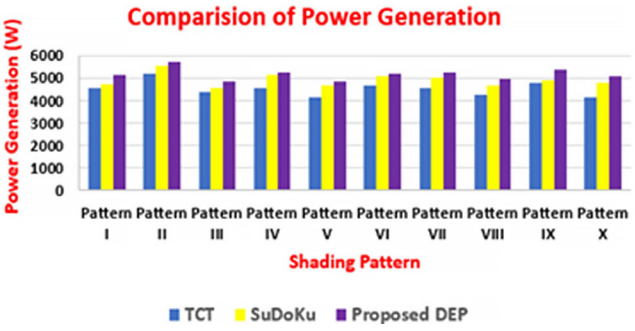

Fig. 24 Comparison of Power Generation

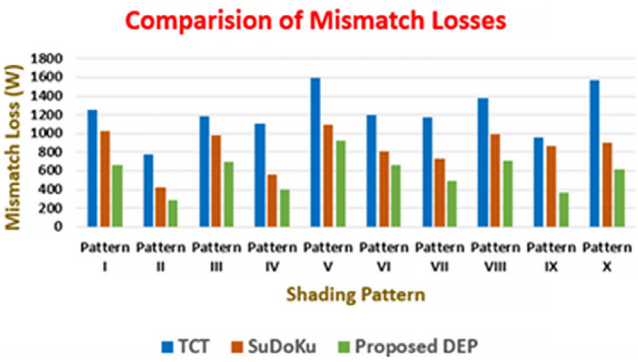

Fig. 25 Comparison of Mismatch Losses

6 Experimental validation

The experimentation has been done using mini solar PV cells rating 384 mW, an open circuit voltage of 2.9 V, a short circuit current of 149.8 mA, a nominal voltage of 2.73 V, and a nominal current of 139.8 mA at STC 1000 W/m^2, 25 °C. Fig. 28 shows the TCT and proposed configuration for 3 × 3 array.

To induce uniform irradiation in the mini solar PV cell, LEDs are used in experimentation of same size and shape.

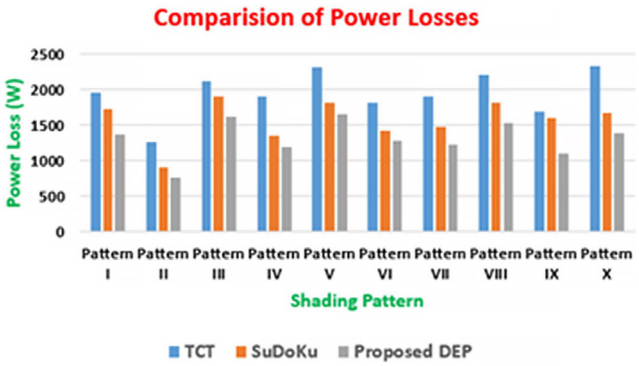

Fig. 26 Comparison of Power Losses

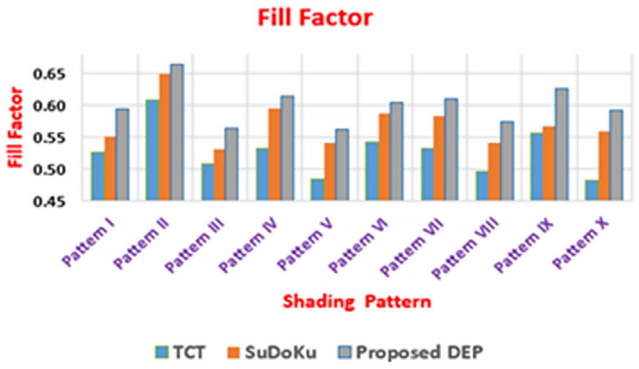

Fig. 27 Fill Factor at ten different Shading Patterns

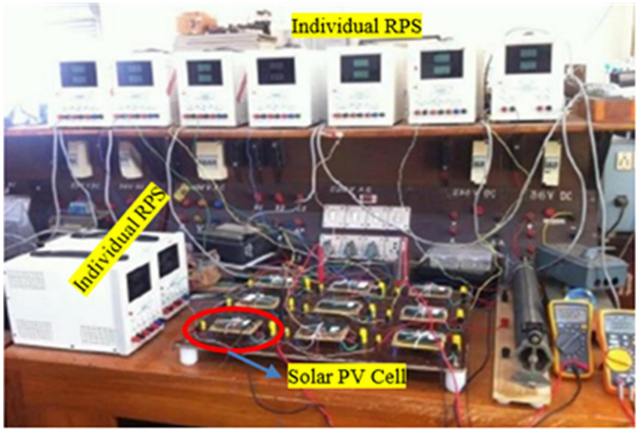

Fig. 28 Experimental setup

The power to each LED is supplied by using a separate regulated power supply. To produce different shade patterns, the voltage applied from individual power supply will change to corresponding LED source.

Here, we are considering the three shading patterns and their insolation values of 1000 W/m^2, 900 W/m^2, 800 W/m^2 and 700 W/m^2 as shown in Fig. 29, the corresponding individual power supply voltages applied to the LEDs are 2.457 V, 2.184 V and 1.911 V respectively.

The experimentation has been conducted to verify the effectiveness of the DEP algorithm at the above stated

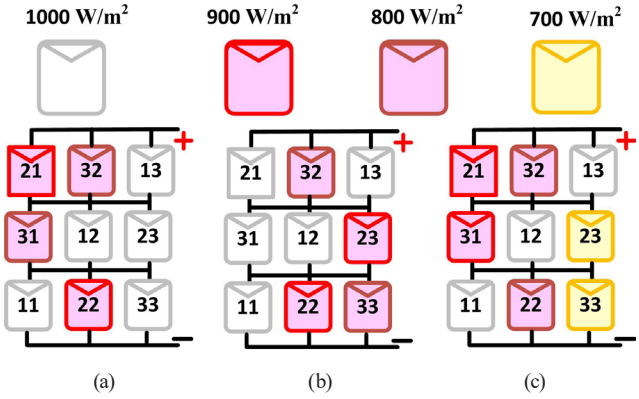

Fig. 29 Experimentation shading patterns of DEP
(a) Pattern I, (b) Pattern II, (c) Pattern III

shading patterns, and it has been in square and rectangular shape. Table 3 shows the comparison of proposed DEP with other stated configurations of basic TCT and SuDoKu.

Fig. 30 shows the comparision of solar PV array power generation and mismatch loss at different experimental shading patterns. From the experimental results, the power enhancement has been observed 3.69%, 3.69% and 4% and mismatch losses are reduced to 49.11%,49.11% and 48.9% with the proposed DEP when compared with basic TCT configuration. The values would be 1.31%, 41.91% for Pattern I, II and 1.41%, 40% for Pattern III when compared with SuDoKu configuration.

From Fig. 31, the comparison of power losses and fill factor has been observed. For Pattern I and II, the power losses are reduced to 30.05% and for Pattern III it is 18.45%. The fill factor with the proposed DEP is increased to 0.79 from 0.76 for Pattern I and II, 0.73 from 0.70 for Pattern III.

Table 3 Power Loss, Fill Factor, Mismatch Loss for three different Shading Patterns

Shading Pattern	Configuration	Power (W)	Mismatch Loss (W)	Power Loss (W)	Fill Factor
Pattern I	TCT	2.98	0.226	0.476	0.76
	Sudoku	3.05	0.198	0.406	0.78
	Proposed DEP	3.09	0.115	0.366	0.79
Pattern II	TCT	2.98	0.226	0.476	0.76
	Sudoku	3.05	0.198	0.406	0.78
	Proposed DEP	3.09	0.115	0.366	0.79
Pattern III	TCT	2.75	0.229	0.706	0.70
	Sudoku	2.82	0.195	0.636	0.72
	Proposed DEP	2.86	0.117	0.596	0.73

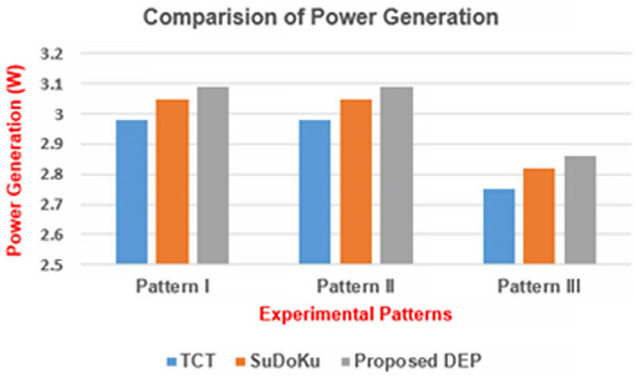

(a)

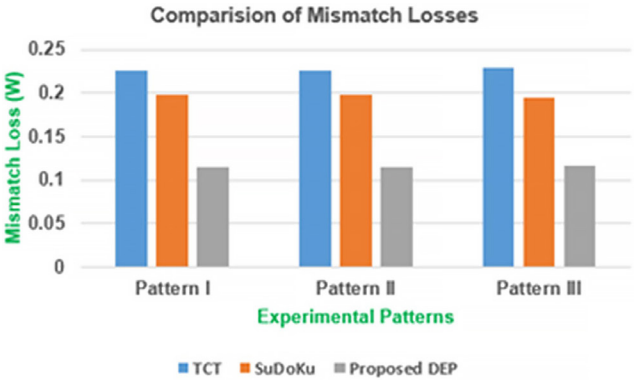

(b)

Fig. 30 Experimental performance comparison of (a) Power Generation, (b) Mismatch Loss

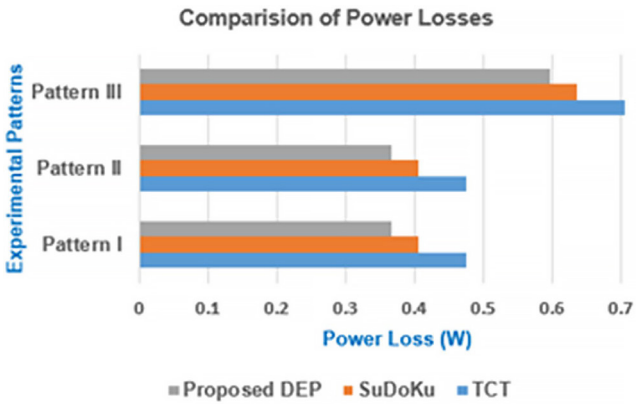

(a)

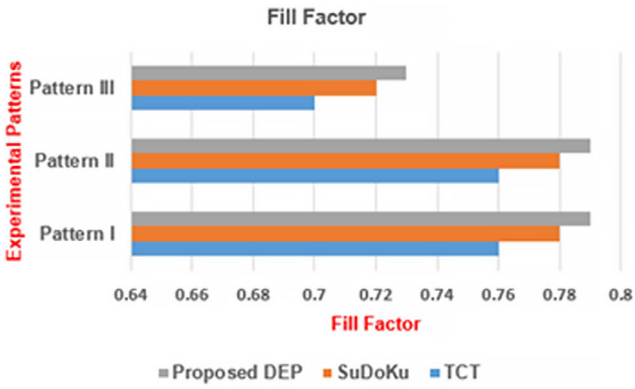

(b)

Fig. 31 Experimental performance comparison of (a) Power Losses, (b) Fill Factor

7 Conclusion

This paper proposes a novel method of DEP algorithm in a shaded photovoltaic (PV) system. This approach aims to address the issue of mismatch power loss, a limitation observed in the existing algorithms available in the literatures. In the proposed approach, the column-based reconfiguration has been done and it is a one-time static reconfiguration for the commonly occurring shading patterns in a location. The DEP is simulated on 9 × 9 PV array using MATLAB/Simulink, an highest power improvement of 23.01% and 10.20% in maximum power were observed when compared with standard TCT and SuDoKu configurations respectively. In terms of power loss, an average of 300 W is reduced with DEP algorithm compared with stated configurations for the adhered patterns. Based on the analysis, it has been proved that, SuDoKu has fairly a better performance ratio in all the patterns when compared with TCT. Unlike the other two configurations, the proposed configuration DEP delivers a highest performance ratio in an average of 5 % for all the implemented patterns. To validate the proposed DEP algorithm, an experimention has been conducted on 3 × 3 PV array at three different shading patterns. Taking all the simulation and experimental results into consideration, it is clear that the DEP arrangement has the least power loss and the best performance ratio when compared with other configurations under all tested shading scenarios.

In future, the proposed technique would be tested experimentally with higher solar PV configurations of 9 × 9, 12 × 12 etc. Also, to implement machine learning models in coordination with DEP for tracing the solar irradiation, shading patterns based on weather forecasts and historical data. Further, the DEP algorithm can be combined with fuzzy logic, GA, or reinforcement learning to improve convergence speed and solution quality and modify the DEP to support dynamic reconfiguration for better real-time adaptability under rapidly changing irradiance. Its application across various domains including smart microgrids, distributed renewable systems, and IoT-integrated energy management, underscores its versatility and practical value.

References

[1] Taghavi, M., Lee, C.-J. "Development of a novel hydrogen liquefaction structure based on liquefied natural gas regasification operations and solid oxide fuel cell: Exergy and economic analyses", Fuel, 384, 133826, 2025. https://doi.org/10.1016/j.fuel.2024.133826

[2] Taghavi, M., Lee, C.-J. "Development of novel hydrogen liquefaction structures based on waste heat recovery in diffusion-absorption refrigeration and power generation units", Energy Conversion and Management, 302, 118056, 2024. https://doi.org/10.1016/j.enconman.2023.118056

[3] Taghavi, M., Yoon, H.-J., Choi, J.-U., Lee, C.-J. "Innovative structure of a Liquefied Natural Gas (LNG) process by mixed fluid cascade using solar renewable energy, Photovoltaic Panels (PV), and absorption refrigeration system", Computer Aided Chemical Engineering, 53, pp. 2071–2076, 2024. https://doi.org/10.1016/B978-0-443-28824-1.50346-X

[4] Taghavi, M., Salarian, H., Ghorbani, B. "Economic evaluation of a hybrid hydrogen liquefaction system utilizing liquid air cold recovery and renewable energies", Renewable Energy Research and Applications, 4(1), pp. 125–143, 2023. https://doi.org/10.22044/rera.2022.11899.1122

[5] Soonmin, H., Taghavi, M. "Solar energy development: Study cases in Iran and Malaysia", International Journal of Engineering Trends and Technology, 70(8), pp. 408–422, 2022. https://doi.org/10.14445/22315381/IJETT-V70I8P242

[6] Ebrahimi, A., Ghorbani, B., Taghavi, M. "Novel integrated structure consisting of CO2 capture cycle, heat pump unit, Kalina power, and ejector refrigeration systems for liquid CO2 storage using renewable energies", Energy Science and Engineering, 10(8), pp. 3167–3188, 2022. https://doi.org/10.1002/ese3.1211

[7] Taghavi, M., Salarian, H., Ghorbani, B. "Thermodynamic and exergy evaluation of a novel integrated hydrogen liquefaction structure using liquid air cold energy recovery, solid oxide fuel cell and photovoltaic panels", Journal of Cleaner Production, 320, 128821, 2021. https://doi.org/10.1016/j.jclepro.2021.128821

[8] Afrouzy, Z. A., Taghavi, M. "Thermoeconomic analysis of a novel integrated structure for liquefied natural gas production using photovoltaic panels", Journal of Thermal Analysis and Calorimetry, 145, pp. 1509–1536, 2021. https://doi.org/10.1007/s10973-021-10769-4

[9] Ahmed, J., Salam, Z. "A critical evaluation on maximum power point tracking methods for partial shading in PV systems", Renewable and Sustainable Energy Reviews, 47, pp. 933–953, 2015. http://doi.org/10.1016/j.rser.2015.03.080

[10] Winston, D. P., Karthikeyan, G., Pravin, M., Jebasingh, O., Akash, A. G., Nithish, S., Kabilan, S. "Parallel power extraction technique for maximizing the output of solar PV array", Solar Energy, 213, pp. 102–117, 2021. https://doi.org/10.1016/j.solener.2020.10.088

[11] Belhachat, F., Larbes, C. "Modeling, analysis and comparison of solar photovoltaic array configurations under partial shading conditions", Solar Energy, 120, pp. 399–418, 2015. http://doi.org/10.1016/j.solener.2015.07.039

[12] Ramaprabha, R., Mathur, B. L. "A comprehensive review and analysis of solar photovoltaic array configurations under partial shaded conditions", International Journal of Photoenergy, 2012(1), 120214, 2012. https://doi.org/10.1155/2012/120214

[13] Dhiman, G., Kumar, V. "Emperor penguin optimizer: A bio-inspired algorithm for engineering problems", Knowledge-Based Systems, 159, pp. 20–50, 2018. https://doi.org/10.1016/j.knosys.2018.06.001

[14] Deshkar, S. N., Dhale, S. B., Mukherjee, J. S., Babu, T. S., Rajasekar, N. "Solar PV array reconfiguration under partial shading conditions for maximum power extraction using genetic algorithm", Renewable and Sustainable Energy Reviews, 43, pp. 102–110, 2015. http://doi.org/10.1016/j.rser.2014.10.098

[15] Babu, T. S., Ram, J. P., Dragičević, T., Miyatake, M., Blaabjerg, F., Rajasekar, N. "Particle swarm optimization based solar PV array reconfiguration of the maximum power extraction under partial shading conditions", IEEE Transactions on Sustainable Energy, 9(1), pp. 74–85, 2018. https://doi.org/10.1109/TSTE.2017.2714905

[16] Fathy, A. "Recent meta-heuristic grasshopper optimization algorithm for optimal reconfiguration of partially shaded PV array", Solar Energy, 171, pp. 638–651, 2018. https://doi.org/10.1016/j.solener.2018.07.014

[17] Yousri, D., Allam, D., Eteiba, M. B. "Optimal photovoltaic array reconfiguration for alleviating the partial shading influence based on a modified Harris hawks optimizer", Energy Conversion and Management, 206, 112470, 2020. https://doi.org/10.1016/j.enconman.2020.112470

[18] Babu, T. S., Yousri, D., Balasubramanian, K. "Photovoltaic array reconfiguration system for maximizing the harvested power using population-based algorithms", IEEE Access, 8, pp. 109608–109624, 2020. https://doi.org/10.1109/ACCESS.2020.3000988

[19] Tabanjat, A., Becherif, M., Hissel, D. "Reconfiguration solution for shaded PV panels using switching control", Renewable Energy, 82, pp. 4–13, 2015. http://doi.org/10.1016/j.renene.2014.09.041

[20] Sanseverino, E. R., Ngoc, T. N., Cardinale, M., Vigni, V. L., Musso, D., Romano, P., Viola, F. "Dynamic programming and Munkres algorithm for optimal photovoltaic arrays reconfiguration", Solar Energy, 122, pp. 347–358, 2015. http://doi.org/10.1016/j.solener.2015.09.016

[21] Yousri, D., Babu, T. S., Beshr, E., Eteiba, M. B., Allam, D. "A robust strategy based on marine predators algorithm for large scale photovoltaic array reconfiguration to mitigate the partial shading effect on the performance of PV system", IEEE Access, 8, pp. 112407–112426, 2020. https://doi.org/10.1109/ACCESS.2020.3000420

[22] Mishra, N., Yadav, A. S., Pachauri, R., Chauhan, Y. K., Yadav, V. K. "Performance enhancement of PV system using proposed array topologies under various shadow patterns", Solar Energy, 157, pp. 641–656, 2017. http://doi.org/10.1016/j.solener.2017.08.021

[23] Horoufiany, M., Ghandehari, R. "Optimization of the Sudoku based reconfiguration technique for PV arrays power enhancement under mutual shading conditions", Solar Energy, 159, pp. 1037–1046, 2018.
http://doi.org/10.1016/j.solener.2017.05.059

[24] Akrami, M., Pourhossein, K. "A novel reconfiguration procedure to extract maximum power from partially-shaded photovoltaic arrays", Solar Energy, 173, pp. 110–119, 2018.
https://doi.org/10.1016/j.solener.2018.06.067

[25] Belhaouas, N., Cheikh, M.-S. A., Agathoklis, P., Oularbi, M.-R., Amrouche, B., Sedraoui, K., Djilali, N. "PV array power output maximization under partial shading using new shifted PV array arrangements", Applied Energy, 187, pp. 326–337, 2017.
http://doi.org/10.1016/j.apenergy.2016.11.038

[26] Pareek, S., Dahiya, R. "Enhanced power generation of partial shaded photovoltaic fields by forecasting the interconnection of modules", Energy, 95, pp. 561–572, 2016.
http://doi.org/10.1016/j.energy.2015.12.036

[27] Satpathy, P. R., Sharma, R., Jena, S. "A shade dispersion interconnection scheme for partially shaded modules in a solar PV array network", Energy, 139, pp. 350–365, 2017.
http://doi.org/10.1016/j.energy.2017.07.161

[28] Krishna, G. S., Moger, T. "Enhancement of maximum power output through reconfiguration techniques under non-uniform irradiance conditions", Energy, 187, 115917, 2019.
https://doi.org/10.1016/j.energy.2019.115917

[29] Nasiruddin, I., Khatoon, S., Jalil, M. F., Bansal, R. C. "Shade diffusion of partial shaded PV array by using odd-even structure", Solar Energy, 181, pp. 519–529, 2019.
https://doi.org/10.1016/j.solener.2019.01.076

[30] MATLAB/Simulink "The MathWorks, Inc., Natick, Massachusetts, USA., (Version 2021a)", [computer program] Available at: https://in.mathworks.com/campaigns/products/trials.html [Accessed: 25 May 2025]